

# ON THE NEUTRAL GAS CONTENT AND ENVIRONMENT OF NGC 3109 AND THE ANTILIA DWARF GALAXY

D. G. BARNES

Centre for Astrophysics & Supercomputing, Mail number 31, Swinburne University of Technology, PO Box 218, Hawthorn, VIC 3122, Australia  
dbarnes@swin.edu.au

W. J. G. DE BLOK

Australia Telescope National Facility, CSIRO, PO Box 76, Epping, NSW 1710, Australia  
edeblok@atnf.csiro.au

*To appear in AJ, 2001.*

## ABSTRACT

As part of a continuing survey of nearby galaxies, we have mapped the neutral gas content of the low surface brightness, Magellanic-type galaxy NGC 3109 — and its environment, including the Antlia dwarf galaxy — at unprecedented velocity resolution and brightness sensitivity. The HI mass of NGC 3109 is measured to be  $(3.8 \pm 0.5) \times 10^8 M_{\odot}$ . A substantial warp in the disk of NGC 3109 is detected in the HI emission image in the form of an extended low surface brightness feature. We report a positive detection in HI of the nearby Antlia dwarf galaxy, and measure its total neutral gas mass to be  $(6.8 \pm 1.4) \times 10^5 M_{\odot}$ . We show the warp in NGC 3109 to lie at exactly the same radial velocity as the gas in the Antlia dwarf galaxy and speculate that Antlia disturbed the disk of NGC 3109 during a mild encounter  $\sim 1$  Gyr in the past. HI data for a further eight galaxies detected in the background are presented.

*Subject headings:* galaxies: individual (NGC 3109, Antlia dwarf)—galaxies: interactions—Local Group

## 1. INTRODUCTION

The morphology and evolution of galaxies are for a major part determined by their environment. Spectacular systems such as the Antennae (Arp 1966; Toomre & Toomre 1972) and the Cartwheel galaxy (Struck-Marcell & Higdon 1993; Higdon 1996) are extreme examples of distortion caused by nearby companions. Locally, the Magellanic Stream offers a close-up view of a system dominated by the gravitational field of the Milky Way Galaxy (Putman et al. 1998). Intense infrared emission appears to be triggered by strong interactions between spirals that are rich in molecular gas (Sanders & Mirabel 1996), and there is evidence that low surface brightness (LSB) galaxies accompanied by nearby dwarf galaxies will be rapidly transformed into star-bursting blue compact galaxies because of tidal effects (Taylor 1997). N-body simulations support the observations, showing galaxy harassment to be capable of transforming disk galaxies into spheroidal galaxies (Moore et al. 1996, 1998a) and perhaps also of seeding quasar formation in massive, low surface brightness disks (Moore et al. 1998b).

Understanding the effects that companions have on their parent galaxies is therefore important in the context of galaxy evolution. While a number of galaxies, especially the Milky Way, are known to be embedded in a halo of dwarf galaxies, very few galaxies are known to have *gravitationally bound* companions. If, as is often claimed, galaxy formation is still on-going (e.g. Wilcots & Miller 1998), many galaxies should still be surrounded by a halo of dwarf galaxies and infalling neutral hydrogen gas (HI) clouds. Occasional serendipitous discoveries have given us tantalising glimpses of these kind of phenomena, such as infalling dwarf galaxies surrounding Magellanic irregulars (Wilcots et al. 1996), and infalling gas clouds in LSB galaxies (de Blok & Walter 2000; de Blok et al. 1999). For

the systems that are known, the dynamics of the infalling dwarf galaxies are an excellent indicator of the presence and mass of dark matter in the parent galaxy, especially since the dwarfs are found out to much larger radii than the galaxy disk (Zaritsky et al. 1997).

To address the lack of information pertaining to companions to known galaxies, we have commenced a deep HI survey of extended regions around selected nearby galaxies. HI observations are ideal for finding gas-rich dwarf companion galaxies, but large volumes near target galaxies have hitherto not been surveyed since HI observations that are both wide-field and sensitive have been too expensive in observing time. The new Parkes 21 cm Multibeam receiver (Staveley-Smith et al. 1996) however, with its narrowband filters (Haynes et al. 1998), offers the opportunity to efficiently image nearby galaxies and their environments at unprecedented brightness sensitivity and velocity resolution, with moderate spatial resolution.

To date, we have imaged the HI environments of four galaxies — Wolf-Lundmark-Melotte (WLM), Sextans A, NGC 1313 and NGC 3109 — using this instrument. Our observations provide lower image noise, finer velocity resolution and fewer observing artifacts than standard HIPASS data (Barnes et al. 2001). The combined results of our survey (including further galaxies) will be the subject of a future paper. In the meantime, this paper reports the findings associated with NGC 3109, a LSB, Magellanic, late-type spiral. A brief description of NGC 3109 and its environment is given in Section 2, followed in Section 3 by a description of the observations. The results of the observations, pertaining to NGC 3109, to background galaxies and to the Antlia dwarf galaxy, are documented in Section 4 and discussed in Section 5.

## 2. NGC 3109

NGC 3109 is a well-studied galaxy at a distance of  $(1.2 \pm 0.1)$  Mpc (Capaccioli et al. 1992; Lee 1993), which places it in the outskirts of the Local Group of galaxies (van den Berg 1994). The radial velocity of the galaxy is  $404 \text{ km s}^{-1}$  (Jobin & Carignan 1990). NGC 3109 has been variously classified as Irr (Sandage 1961; van den Berg 1994), Sm (Sandage & Tammann 1987) and SB(s)m (de Vaucouleurs et al. 1991). In this paper, we consider NGC 3109 to be a LSB, Magellanic, late-type galaxy seen edge-on at an inclination of  $75^\circ$  to  $80^\circ$  (Carignan 1985; Jobin & Carignan 1990).

NGC 3109 appears to be dark-matter dominated, having a dark-to-luminous mass ratio of 5–10 (Jobin & Carignan 1990). Stars in the disk of NGC 3109 have ages as young as  $10^7$  yr, and a halo of Population II stars with ages exceeding  $10^{10}$  yr has been observed (Minniti et al. 1999). This is consistent with models of LSB galaxies which exhibit star formation rates that are on average low but erratic (e.g. Gerritsen & de Blok 1999). Since these galaxies evolve slowly, the surrounds of NGC 3109 may be relatively rich in agglomerations of HI whose densities have not reached those required for star formation, and which have not yet settled into the disk of the galaxy.

Already, one possible companion to NGC 3109 is known: the Antlia dwarf galaxy (hereafter, Antlia), at a distance of  $(1.3 \pm 0.1)$  Mpc from the Milky Way (Sarajedini et al. 1997; Aparicio et al. 1997). Like NGC 3109, Antlia contains stellar populations of all ages (Sarajedini et al. 1997), with most recent star formation taking place slowly in the central regions (Aparicio et al. 1997). In this respect, it is typical of the dwarf spheroidals in the Local Group (e.g. Tucana, Carina). The radial velocity of Antlia is  $361 \text{ km s}^{-1}$  (Fouqué et al. 1990). Aparicio et al. (1997) calculate the physical separation of NGC 3109 and Antlia to be between 29 kpc and 180 kpc, with a maximum separation of 37 kpc for the pair to be gravitationally bound.

### 3. OBSERVATIONS

We have acquired a deep HI image of a field 120 kpc square centered on NGC 3109 and including Antlia. Our observations utilise the new 21 cm Multibeam system at the prime focus of the Parkes 64 m radiotelescope.<sup>1</sup> With narrowband filters installed, the instantaneous observing bandwidth is 8 MHz, which is correlated into 2048 channels for two products XX and YY. We centered the observing band at 1418.4 MHz, corresponding to a radial velocity of  $424 \text{ km s}^{-1}$ , with channels extending  $844 \text{ km s}^{-1}$  either side in increments of  $0.83 \text{ km s}^{-1}$ .

To image NGC 3109 and its surroundings, scans at a rate of  $1^\circ \text{ min}^{-1}$  were made separately in the Declination and Right Ascension directions, across a square field of side length  $5.67^\circ$ . Adjacent scans were separated by a maximum of  $4'$ , so that each beam of the Multibeam system sampled the HI sky at better than the Nyquist rate of the beam. A total of 208 scans were made, comprising  $\sim 200000$  single-polarisation spectra. The individual spectra, recorded every 5 s, were bandpass-corrected, calibrated and imaged using the software developed for the HI Parkes All Sky Survey (HIPASS, Barnes et al. 2001), with the HIPASS parameters slightly modified to accom-

modate the shorter scan length of this survey. The final image, having pixels of side length  $4'$  spatially and  $0.83 \text{ km s}^{-1}$  spectrally, had an RMS noise level of 34 mJy. The image beam (resolution) is  $\sim 15.5'$  FWHM spatially, and  $1.12 \text{ km s}^{-1}$  FWHM spectrally.

## 4. RESULTS

### 4.1. The HI Content of NGC 3109

The spectrum of HI emission integrated spatially over NGC 3109 is shown in Figure 1. The overall profile shape is markedly asymmetric, having a surplus of flux in the lower velocity component of the disk. This property of NGC 3109 has already been noted by Huchtmeier et al. (1980), and will be discussed below. The line centre is located at  $(403.0 \pm 0.2) \text{ km s}^{-1}$ , being the coincident midpoint of the 20% and 50% peak flux points on the edges of the profile. This is in excellent agreement with all previously published values, e.g.  $(404 \pm 2) \text{ km s}^{-1}$  measured by Jobin & Carignan (1990) and  $(403 \pm 2) \text{ km s}^{-1}$  measured by Huchtmeier (1973). The flux-weighted mean velocity is  $(399.5 \pm 0.5) \text{ km s}^{-1}$ , and the peak flux is detected at  $362 \text{ km s}^{-1}$ . The peak projected rotation velocity of the galaxy is  $(72.4 \pm 0.5) \text{ km s}^{-1}$ .

The integrated HI flux of NGC 3109, measured by the traditional zeroth-order moment of the spectrum, and verified with an equivalent but robust statistic, is  $1110_{-30}^{+90} \text{ Jy km s}^{-1}$ ; the uncertainty in this value is dominated by the uncertainty in the image beam (see Barnes et al. 2001). This value compares well to  $1150 \text{ Jy km s}^{-1}$  measured from standard HIPASS data, and is also recovered when the narrowband spectral data is re-imaged in the traditional way (i.e. with a Gaussian smoothing kernel and using the mean estimator instead of the median). Compared to the spectrum published by Jobin & Carignan (1990), from which an integrated HI flux of  $(650 \pm 130) \text{ Jy km s}^{-1}$  is measured, we detect substantially more flux in NGC 3109 at all velocities. This is expected, since Jobin & Carignan (1990) used the Very Large Array (VLA) in a configuration blind to emission on scales much greater than  $\sim 20'$  on the sky. Of the many single dish studies made of NGC 3109, the flux measured here is consistent only with the value  $(1280 \pm 150) \text{ Jy km s}^{-1}$ , measured by Epstein (1964) with the Harvard 60-ft antenna, whose beam is sufficiently large to “see” all of NGC 3109. Other single dish measurements, viz.  $530 \text{ Jy km s}^{-1}$  (Whiteoak & Gardner 1977),  $1390 \text{ Jy km s}^{-1}$  (Dean & Davies 1975),  $1460 \text{ Jy km s}^{-1}$  (Huchtmeier 1973) and  $1660 \text{ Jy km s}^{-1}$  (Huchtmeier et al. 1980), were made using larger telescopes, and we suggest that these measurements have been compromised by large scale insensitivity.

We deduce an HI mass for NGC 3109 of  $(3.8 \pm 0.5) \times 10^8 M_\odot$ , not corrected for HI line opacity. This is lower than most previously determined values for the following reasons: there has been a general trend towards lower distance estimates to NGC 3109 in the more recent literature; the majority of previous HI flux measurements seem too high as described above; no correction of HI optical depth has been made in this work. The synthesis HI mass of Jobin & Carignan (1990), corrected for the recent (lower)

<sup>1</sup> The Parkes radiotelescope is part of the Australia Telescope which is funded by the Commonwealth of Australia for operation as a National Facility managed by CSIRO.

distance measures to NGC 3109, is  $(2.2 \pm 0.5) \times 10^8 M_\odot$ . Thus the HI mass not detected by the VLA observations is of order  $1.6 \times 10^8 M_\odot$ .

In Figure 2, integrated HI column density and flux-weighted velocity maps of NGC 3109 are given. A warp in the column density and velocity field is evident in the south west of the galaxy. Inspection of individual channel maps demonstrates that this component is the source of the asymmetry in the (single dish) integrated HI profile of the galaxy, and that it contains a substantial fraction of the neutral gas not seen by the VLA, in the form of a smooth, extended component near velocity  $360 \text{ km s}^{-1}$ . We note that this reservoir of gas lies in that part of velocity space which coincides with the radial velocity of Antlia. This will be discussed further below.

#### 4.2. Background galaxies

The field imaged by our observations measures 120 kpc square at a distance of 1.2 Mpc. As expected, the Antlia dwarf galaxy was detected, and its HI parameters are presented below. Besides NGC 3109 and Antlia, eight previously catalogued galaxies were detected in the field, at radial velocities between  $\sim 850 \text{ km s}^{-1}$  and  $1150 \text{ km s}^{-1}$ . Data pertaining to these galaxies — including the HI properties measured in this survey — are given in Table 1. Two of the galaxies — NGC 3113 and ESO 499- G037 — have previously been identified as members of the galaxy group LGG 189 (Garcia 1993). The radial velocities of LGG 189 and of the remaining HI galaxies in the field range places them at least  $\sim 12 h_{75}^{-1}$  Mpc behind NGC 3109 and Antlia, allowing us to conclude that it is highly unlikely that they have exerted any influence on the formation or evolution of NGC 3109.

#### 4.3. The HI Content of the Antlia Dwarf Galaxy

The HI emission spectrum extracted at the position of the Antlia dwarf galaxy and integrated over a region  $20' \times 20'$ , is shown in Figure 3. The galaxy is easily detected, and is well distinguished from NGC 3109 emission. The spectrum is that of a single peak profile with a maximum flux of 100 mJy at  $360 \text{ km s}^{-1}$ . The peak flux measured here is consistent with the previously determined upper limits of 150 mJy (Gallagher et al. 1995) and 122 mJy (Fouqué et al. 1990). The line centre is measured to be  $(362.0 \pm 2.0) \text{ km s}^{-1}$ , this being the mean of the midpoints of the 20% and 50% peak flux points on the edges of the profile, in exact agreement with the detection by Fouqué et al. (1990), and coinciding with the flux-weighted mean velocity. The velocity width is  $(30 \pm 2) \text{ km s}^{-1}$ . We note that the detection by Fouqué et al. (1990) is almost certainly real, contrary to the suggestion of Blitz & Robishaw (2000) that it is an instrumental artifact.

Summing the flux in the HI profile of Antlia yields a total flux of  $(1.7 \pm 0.1) \text{ Jy km s}^{-1}$ . Under the usual assumptions, and adopting a distance of  $(1.3 \pm 0.1) \text{ Mpc}$  to Antlia, this yields an HI mass of  $(6.8 \pm 1.4) \times 10^5 M_\odot$ . Our result is considerably lower than that of Whiting et al. (1997), who used the data of Fouqué et al. (1990) to determine a total HI mass of Antlia of order  $(1.0 \pm 0.2) \times 10^6 M_\odot$ ,<sup>2</sup> and lies within the range of HI contents detected in dwarf

spheroidal galaxies by Blitz & Robishaw (2000). Moment analysis applied to the HI spectrum of Antlia yields a line-of-sight RMS velocity of  $6.4 \pm 0.7 \text{ km s}^{-1}$ . Following Whiting et al. (1997), a central mass-to-light ratio of  $(7.6 \pm 1.6) M_\odot / L_\odot$  is calculated for Antlia.

### 5. DISCUSSION

#### 5.1. Sensitivity

For a point source at the distance of NGC 3109, the minimum detectable HI mass ( $3\sigma$  per channel) is of order  $4 \times 10^4 \Delta V M_\odot$  where  $\Delta V$  is the velocity width of the galaxy expressed in  $\text{km s}^{-1}$ . We have neglected the improvement in detectability as source width increases, and so the Antlia dwarf galaxy, which extends over more than 30 channels, actually lies slightly below this limit. For a smooth distribution of HI filling the beam, the minimum detectable column density for these observations is  $10^{17} \text{ cm}^{-2}$  ( $3\sigma$ , per  $0.83 \text{ km s}^{-1}$  channel). Such a gas cloud would have a neutral gas mass similar to that calculated for the point source case.

#### 5.2. Dwarf galaxy populations

In the cube of space centred on NGC 3109, with side-length 120 kpc, we have detected only one dwarf galaxy — Antlia. No other isolated reservoirs of neutral gas were found, and so at this point little can be deduced about the dark matter content of NGC 3109 and its surrounds. To escape detection, a gas cloud in the vicinity of NGC 3109 could be:

1. spatially extended but have a neutral gas column density less than  $\sim 10^{17} \text{ cm}^{-2}$ ,
2. smaller in spatial extent than  $\sim 4 \text{ kpc}$  and less massive than  $\sim 4 \times 10^4 \Delta V M_\odot$ , or be
3. unresolved from NGC 3109.

Objects in the first category are exceedingly difficult to detect without committing substantial telescope time, and even then will likely be invisible in HI emission given the typical column density cutoff seen in galaxy disks at  $2 \times 10^{19} \text{ cm}^{-2}$  (Corbelli & Salpeter 1993). Nevertheless, such objects must surely exist as a component of the Ly alpha absorber population.

Dwarf galaxies bound to NGC 3109 will primarily fall into the second and third categories. Further HI imaging at higher spatial resolution can be used to search for gas clouds unresolved from NGC 3109 (category three), but the Parkes 21 cm Multibeam remains the best instrument for finding the low HI mass objects of category two.

Our findings are consistent with other recent searches for extremely low HI mass objects. For example, the Arecibo HI strip survey of Zwaan & Briggs (2000) yielded an HI mass function predicting a number density of  $\sim 2 \text{ Mpc}^{-3}$  for objects having HI masses in the decade  $10^{4.5} - 10^{5.5} M_\odot$ . This gives a detection probability of  $\sim 0.5$  per cent for a single object in this mass range in the present study of  $2 \times 10^{-3} \text{ Mpc}^3$ .

<sup>2</sup> We have corrected their result for our adopted distance to Antlia.

### 5.3. NGC 3109 and Antlia

The warp of the gas disk of NGC 3109 detected here is also suggested in the data of Jobin & Carignan (1990). Their Figure 4 shows a narrow plume of low column density gas extending  $\sim 5$  kpc southwest from the disk. Our observations suggest that the gas plume is sitting on top of a more massive but smooth distribution of HI which is invisible to the synthesis observations. Jobin & Carignan (1990) note that the HI plume, together with the slight southwest displacement of the optical isophotes, is suggestive of a past interaction with another system, yet are unable to suggest a suitable nearby system. Since the plume (or warp) lies at exactly the radial velocity of Antlia, we speculate that Antlia is this very companion, and that some mild interaction has occurred between NGC 3109 and Antlia in the distant past.

For a current separation of  $\sim 50$  kpc, and a differen-

tial velocity of  $\sim 50$  km s $^{-1}$ , an interaction may have taken place  $\sim 1$  Gyr ago. The encounter would need to have been prolonged enough to draw out a substantial mass of neutral gas (of order  $10^8 M_\odot$ ) but mild so as not to cause massive star formation – the plume is presently undetected optically. Recent n-body simulations of the Milky Way and Magellanic Clouds (e.g. Yoshizawa 1998) have shown that such encounters can occur. Further N-body simulations of the NGC 3109 and Antlia system are needed to assess whether this proposed past encounter is feasible.

We are grateful to the staff of the Parkes observatory – in particular John Reynolds and Mal Smith – for their expert assistance during the observations. We are also grateful for the continuing support of the LIVEDATA software by Mark Calabretta and Lister Staveley-Smith of the Australia Telescope National Facility.

### REFERENCES

- Arp, H. 1966, *ApJS*, 14, 1  
 Aparicio, A., Dalcanton, J. J., Gallart, C., & Martínez-Delgado, D. 1997, *AJ*, 114, 1447  
 Barnes, D. G., et al. 2001, *MNRAS*, 322, 486  
 Blitz, L., & Robishaw, T. 2000, *ApJ*, 541, 675  
 Capaccioli, M., Piotto, G., & Bresolin, F. 1992, *AJ*, 103, 1151  
 Carignan, C. 1985, *ApJ*, 299, 59  
 Corbelli, E., Salpeter, E. E. 1993, *ApJ*, 419, 104  
 de Blok, W. J. G., Walter, F. 2000, *ApJ*, 537, L95  
 de Blok, W. J. G., Walter, F., & Bell, E. F. 1999, *Ap&SS*, 269, 101  
 de Vaucouleurs, G., et al. 1991, *Third Reference Catalogue of Bright Galaxies* (New York: Springer)  
 Dean, J. F., & Davies, R. D. 1975, *MNRAS*, 170, 503  
 Epstein, E. E. 1964, *AJ*, 69, 490  
 Fouqué, P., Bottinelli, L., Durand, N., Gouguenheim, L., & Paturel, G. 1990, *A&AS*, 86, 473  
 Gallagher II, J. S., Littleton, J. E., & Matthews, L.D. 1995, *AJ*, 109, 2003  
 Garcia, A. M. 1993, *A&AS*, 100, 470  
 Gerritsen, J. P. E., & de Blok, W. J. G. 1999, *A&A*, 342, 655  
 Haynes, R. F., et al. 1998, in *IAU Symp. 190, New Views of the Magellanic Clouds*, ed. Y.-H. Chu, N. Suntzeff, J. Hesser, & D. Bohlender (City :publisher), 63  
 Higdon, J. L. 1996, *ApJ*, 467, 241  
 Huchtmeier, W. K. 1973, *A&A*, 22, 27  
 Huchtmeier, W. K., Seiradakis, J. H., & Materne, J. 1980, *A&A*, 91, 341  
 Jobin, M., & Carignan, C. 1990, *AJ*, 100, 648  
 Lee, M. G. 1993, *ApJ*, 408, 409  
 Minimite, D., Zijlstra, A. A., & Alonso, M. V. 1999, *AJ*, 117, 881  
 Moore, B., Katz, N., Lake, G., Dressler, A., Oemler Jr., A. 1996, *Nature*, 379, 613  
 Moore, B., Lake, G., & Katz, N. 1998a, *ApJ*, 495, 139  
 Moore, B., Lake, G., & Katz, N. 1998b, *ApJ*, 495, 152  
 Putman, M. E., et al. 1998, *Nature*, 394, 752  
 Sandage, A. 1961, *The Hubble Atlas of Galaxies* (Washington, D.C.: Carnegie Institution of Washington)  
 Sandage, A., & Tammann, G. A. 1987, *A Revised Shapley-Ames Catalog of Bright Galaxies* (Washington, D.C.: Carnegie Institution of Washington)  
 Sanders, D. B., & Mirabel, I. F. 1986, *ARA&A*, 34, 749  
 Sarajedini, A., Claver, C. F., & Ostheimer, J. C. Jr. 1997, *AJ*, 114, 2505  
 Staveley-Smith, L., et al. 1996, *PASA*, 13, 243  
 Struck-Marcell, C., & Higdon, J. L. 1993, *ApJ*, 411, 108  
 Taylor, C. L. 1997, *ApJ*, 480, 542  
 Toomre, A., & Toomre, J. 1972, *ApJ*, 178, 623  
 van den Bergh, S. 1994, *AJ*, 107, 1328  
 Whiteoak, J. B., & Gardner, F. F. 1977, *Aust. J. Phys.*, 30, 187  
 Whiting A. B., Irwin, M. J., & Hau, G. K. T. 1997, *AJ*, 114, 996  
 Wilcots, E. M., & Miller, B. W. 1998, *AJ*, 116, 2363  
 Wilcots, E. M., Lehman, C., & Miller, B. W. 1996, *AJ*, 111, 1575  
 Yoshizawa, A. 1998, PhD Thesis, Tohoku University  
 Zaritsky, D., Smith, R., Frenk, C., & White, S. D. M. 1997, *ApJ*, 478, 39  
 Zwann, M. A., & Briggs, F. H. 2000, *ApJ*, 530, L61

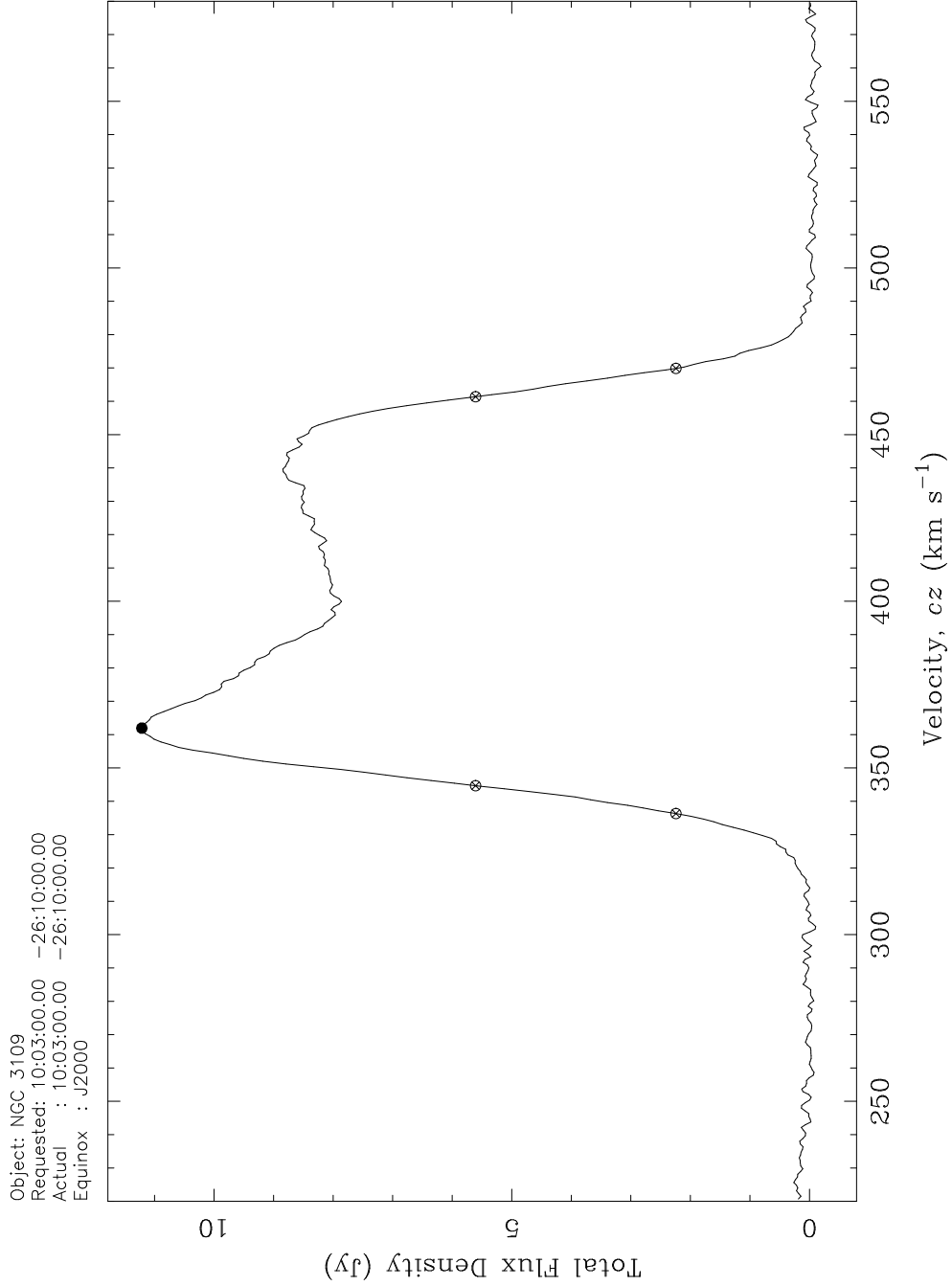


FIG. 1.— The integrated HI profile of NGC 3109, smoothed with a Hanning filter of width three channels. The 50% and 20% peak flux points are marked (width-minimised points with crosses, width-maximised with hollow circles), along with the peak flux itself (solid circle) at  $362 \text{ km s}^{-1}$ .

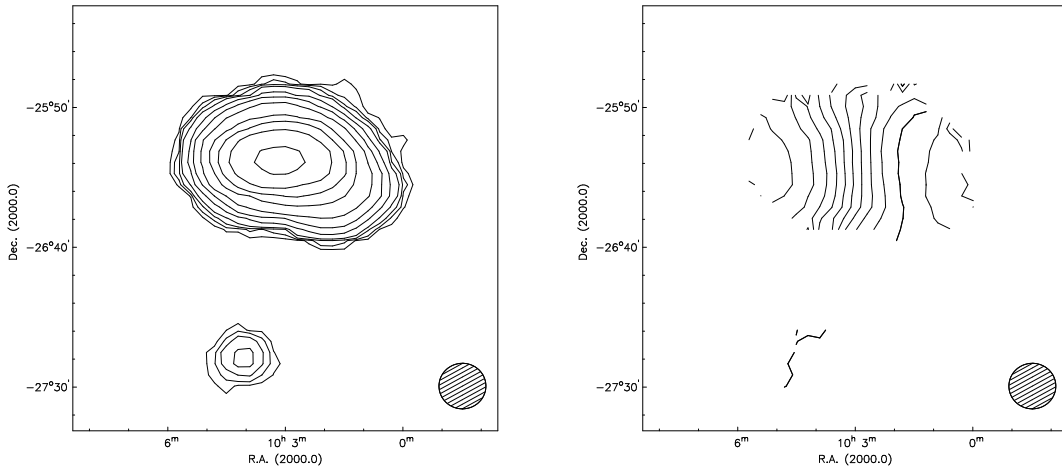


FIG. 2.— Integrated HI column density map (left) and velocity field (right) of NGC 3109 and the Antlia dwarf galaxy. The column density contours are placed at 2, 5, 10, 20, 50, 100, 200, 500, 1000, 2000 and  $5000 \times 10^{17} \text{ cm}^{-2}$ . The velocity contours increase by  $10 \text{ km s}^{-1}$  eastward, and the bold contour lies at  $360 \text{ km s}^{-1}$ . The approximate observing beam size is given at the lower right of each map.

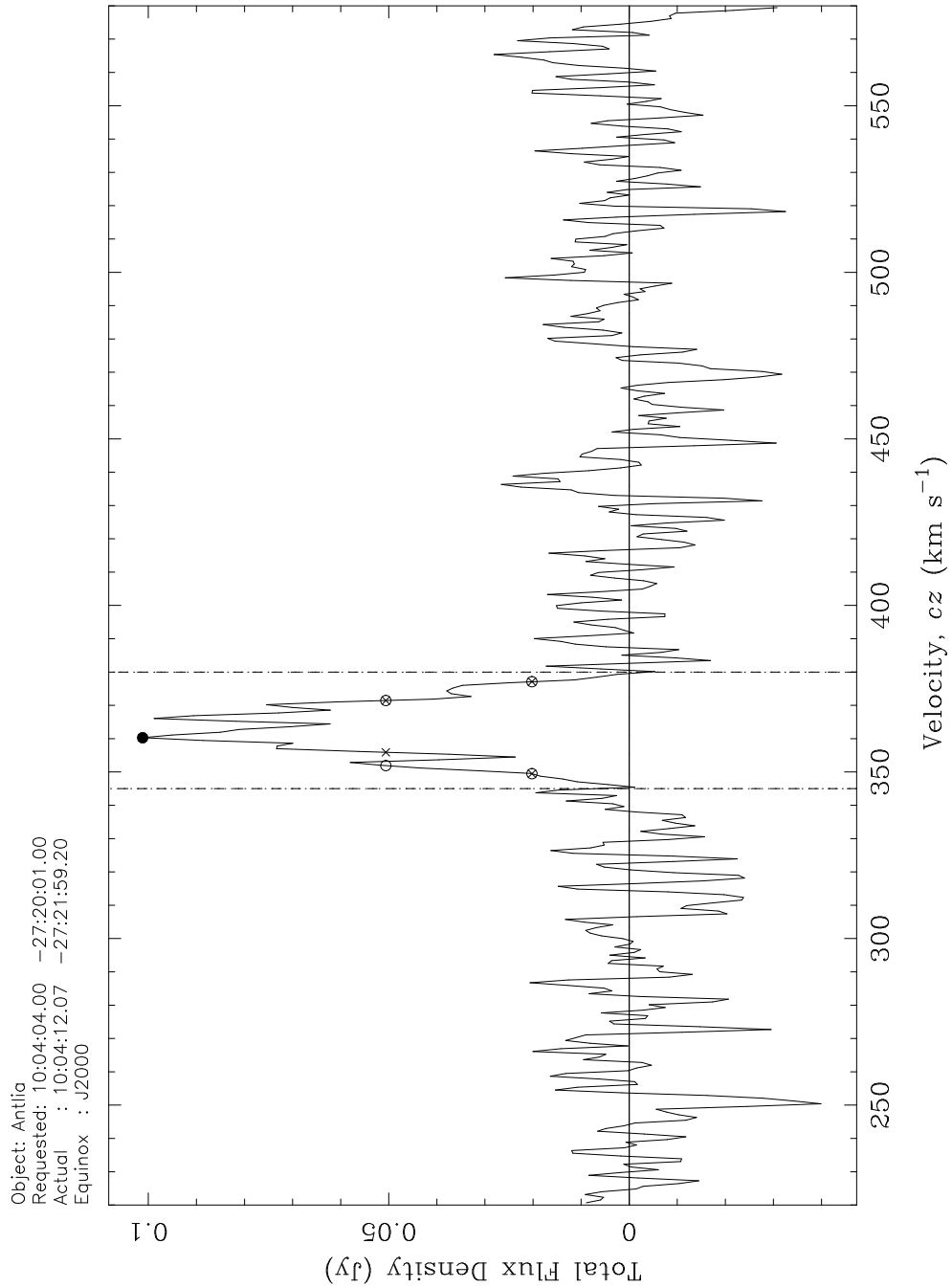


FIG. 3.— An HI spectrum taken at the position of the Antlia dwarf galaxy, integrated over an area  $20'$  square, and smoothed with a Hanning filter three channels wide. The baseline was removed with a seventh order fit to the channels exterior to the region marked by the dashed lines. The 50% and 20% peak flux points are marked as for Figure 1, as is the peak flux itself at  $360 \text{ km s}^{-1}$ .

TABLE 1  
HI DETECTIONS IN THE NGC 3109 FIELD.

Source	R.A. (J2000)	Dec	Mag (Cousins B <sub>T</sub> )	Line centre (km s <sup>-1</sup> )	Line width (km s <sup>-1</sup> )	HI flux (Jy km s <sup>-1</sup> )	HI mass (M <sub>⊙</sub> )
ESO 499- G010 (N3037)	09:51:24	-27:00:36	13.7	877 ± 3	96 ± 3	7.0 <sup>+ 0.6</sup> <sub>- 0.2</sub>	(2.3 ± 0.3) × 10 <sup>8</sup>
ESO 435- G007 (N3056)	09:54:33	-28:17:55	12.6	969 ± 1	272 ± 2	46 <sup>+ 4</sup> <sub>- 1</sub>	(1.8 ± 0.2) × 10 <sup>9</sup>
ESO 435- G016	09:58:47	-28:37:22	13.4	975 ± 1	150 ± 1	33.2 <sup>+ 2.7</sup> <sub>- 0.9</sub>	(1.3 ± 0.2) × 10 <sup>9</sup>
ESO 435-IG020	09:59:21	-28:07:54	14.4	978 ± 3	112 ± 4	7.8 <sup>+ 0.6</sup> <sub>- 0.2</sub>	(3.1 ± 0.4) × 10 <sup>8</sup>
ESO 499- G036 (N3109)	10:03:07	-26:09:32	10.3	403 ± 1	144 ± 1	1110 <sup>+90</sup> <sub>-30</sub>	(3.8 ± 0.5) × 10 <sup>8</sup>
ESO 499- G037	10:03:42	-27:01:40	13.3	955 ± 1	212 ± 1	49 <sup>+ 4</sup> <sub>- 1</sub>	(1.9 ± 0.3) × 10 <sup>9</sup>
ESO 499- G038	10:03:50	-26:36:46	15.7	888 ± 3	104 ± 2	11.4 <sup>+ 1.0</sup> <sub>- 0.3</sub>	(3.8 ± 0.5) × 10 <sup>8</sup>
Antlia Dwarf Galaxy	10:04:04	-27:20:01	—	362 ± 2	30 ± 2	1.7 <sup>+ 0.2</sup> <sub>- 0.1</sub>	(6.8 ± 1.4) × 10 <sup>5</sup>
ESO 435- G035 (N3113)	10:04:26	-28:26:35	13.4	1082 ± 1	226 ± 1	40 <sup>+ 4</sup> <sub>- 1</sub>	(2.0 ± 0.3) × 10 <sup>9</sup>
ESO 435- G047	10:09:07	-29:03:51	12.2	1105 ± 1	268 ± 1	154 <sup>+12</sup> <sub>- 4</sub>	(7.9 ± 1.0) × 10 <sup>9</sup>

Note. — For N3109 and Antlia, HI masses have been determined using distances as cited in Section 2; for all other galaxies mass calculations Hubble distances have been used with  $H_0 = 75$  km s<sup>-1</sup> Mpc<sup>-1</sup>.